

A Novel Two Switch Non-inverting Buck-Boost Converter based Maximum Power Point Tracking System

Khandker Tawfique Ahmed, Mithun Datta, Nur Mohammad

Departement of Electrical and Electronic Engineering, Chittagong University of Engineering & Technology (CUET), Chittagong, Bangladesh

Article Info

Article history:

Received Apr 11, 2013

Revised May 28, 2013

Accepted Jul 4, 2013

Keyword:

Solar Photovoltaic

MPPT

Buck-boost converter

P & O algorithm

Non-inverting mode

SIMULINK

ABSTRACT

A solar module can't transfer maximum power to the load itself due to impedance mismatch. A maximum power point tracking (MPPT) system could be employed to have the maximum power. A new MPPT system has been developed using Buck-Boost type DC-DC converter. The system is highly efficient and robust. PIC16F73 microcontroller has been used to control the DC-DC converter output. PV module output power is measured using microcontroller. The output power is compared with the previous module output power and the duty cycle of the converter is adjusted continuously to track MPP. This process repeats until the output power reaches near to the maximum power point. In this paper, a maximum power point tracking (MPPT) system is developed using two-switch non-inverting buck-boost converter. Perturb and observe (P & O) MPPT algorithm is used to transfer maximum power from the PV panel which is executed using a microcontroller.

Copyright © 2013 Institute of Advanced Engineering and Science.

All rights reserved.

Corresponding Author:

Nur Mohammad,

Departement of Electrical and Electronic Engineering,

Chittagong University of Engineering & Technology,

Chittagong-4349.

Email: nureee_rueta@yahoo.com

1. INTRODUCTION

Recently, global warming becomes an environmental issue which is due to deposition of huge carbon dioxide and breaking of ozone layer by green house gasses. It was agreed by the developed countries that they would reduce at least 5% of their green house gasses compared to the year 1990 by the year 2012 [1]. Also global power crisis and need for sustainable energy systems forces the development of power supply structures that are based on renewable resources. Photovoltaic (PV) system is gaining popularity among the renewable resources due to advantages such as absence of fuel cost, low maintenance cost and no wear and tear due to absence of moving parts. But still the high installation cost and low energy conversion efficiency hinder the mass use of PV systems. The output power of a PV panel depends on the operating terminal voltage. The maximum power generated by the system changes with the change in insolation and temperature. To increase the output power it is important that the PV panel operates at maximum power point (MPP). The power we extract from the PV module is a dc power. So if the maximum power point is to be tracked by changing the voltage of the PV module there should be a dc-dc converter. There are different topology of dc-dc converter like buck converter, boost converter, buck-boost converter, cuk converter, SEPIC (Single Ended primary Inductance Converter) etc. A buck converter can transfer energy to load at lower voltage than the source voltage. Boost converter transfer energy to load at higher voltage than the source voltage. Buck-boost, CUK, SEPIC can transfer energy to load above and below the source voltage. Buck converter used in MPPT can't pull output voltage greater than that of input voltage. Boost converter used in MPPT can't pull output voltage below input voltage. Buck-boost and CUK converter have inverted

output. These problems are solved by using non-inverting buck-boost converter. The ability to work over a wide range of input voltage to generate both higher and lower voltages while supplying high current makes this topology an attractive choice [2]. Another advantage of non-inverting buck-boost converter is that it has a capacity for extra current storage in the inductor [3].

A non-inverting buck-boost converter is used in the MPPT system in this experiment. The P & O method was implemented using PIC16F73, a robust microcontroller.

2. PV MODULE & ARRAY CHARACTERISTICS

Basically, PV cell is a p-n junction. When light incident on the pn junction of the solar cell, electron hole pair is generated in the depletion layer of solar cell. So if a load is connected to the terminal of solar cell, the excess charges i.e. a current flow through the load. A solar cell can be represented by a current source parallel with a diode, a high resistance and series with a small resistance as shown in Figure 1.

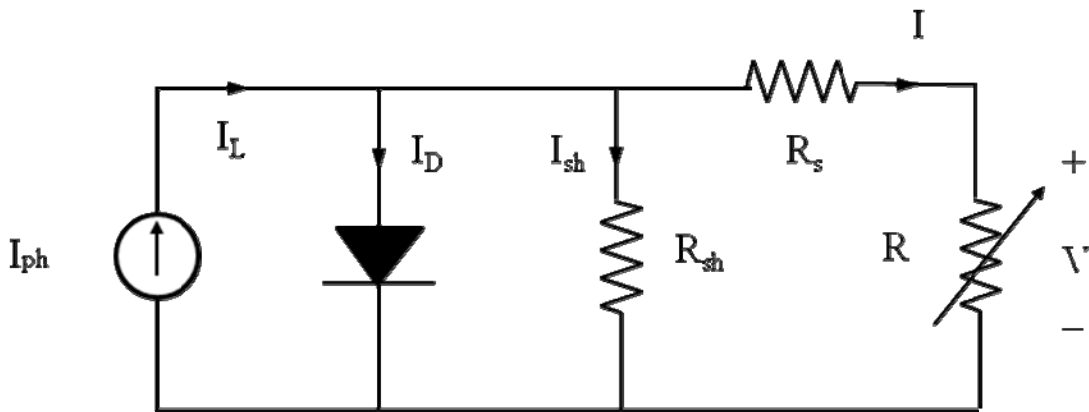


Figure 1. Equivalent circuit of solar cell

PV modules and arrays are built with combined series-parallel configuration of solar cells as shown in Figure 2.

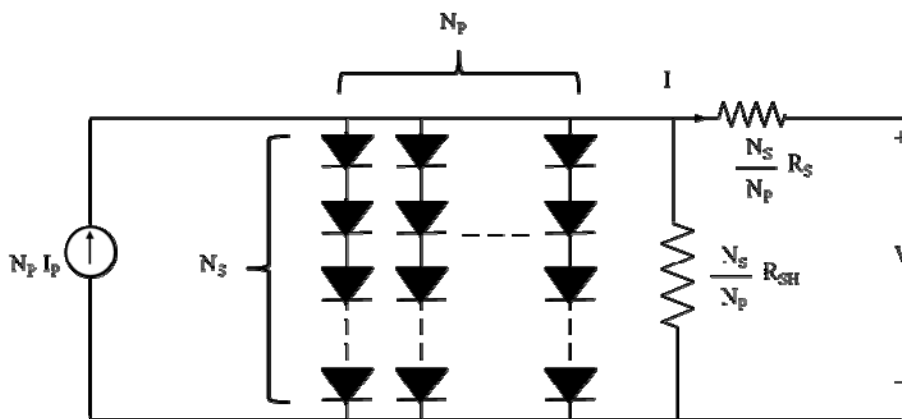


Figure 2. Equivalent circuit of PV module/arrays

The terminal equation for current and voltage of the array becomes [4]-[7]

$$I = N_p I_{PH} - N_p I_S \left[\exp \left(\frac{q(V/N_s + IR_s)}{N_p K T_c A} \right) - 1 \right] - \frac{N_p V}{N_s} + IR_s \tag{1}$$

The photocurrent mainly depends on the solar cell's working temperature

$$I_{PH} = [I_{SC} + K_1(T_C - T_{ref})]A \quad (2)$$

On the other hand, the cell's saturation current varies with cell temperature, which is described as

$$I_S = I_{RS} \left(\frac{T_C}{T_{ref}} \right)^3 \exp \left[\frac{qE_G \left(\frac{1}{T_{ref}} - \frac{1}{T_C} \right)}{kA} \right] \quad (3)$$

Since normally $I_{ph} \gg I_S$ and ignoring the small diode and ground-leakage currents under zero terminal voltage, the short circuit current I_{sc} is approximately equal to the photocurrent I_{ph} , i.e.,

$$I_{PH} = I_{SC} \quad (4)$$

On the other hand, the V_{oc} parameter is obtained by assuming the output current is zero. Given the PV open-circuit voltage V_{oc} at reference temperature and ignoring the shunt leakage current, the reverse saturation current at reference temperature can approximately obtained as

$$\frac{I_{SC}}{\left[\exp \left(\frac{qV_{OC}}{N_S K T_C A} \right) - 1 \right]} \quad (5)$$

In addition, the maximum power can be expressed as.

$$P_{max} = V_{max} i_{max} = \gamma V_{OC} I_{SC} \quad (6)$$

Solar module SOLEREX MSX40 is used in this experiment. The key specifications of this module are shown in table 1.

Table 1. The specifications of the solar module [8]

Model Parameters	Specification MSX40 SOLEREX
Open circuit voltage (V_{oc})	21.1V
Short circuit current (I_{sc})	2.53A
Maximum power (P_{mp})	29.6 W
Voltage at maximum power (V_{mp})	17.2V
Current at maximum power (I_{mp})	2.37A
AM	1.5
Cell temperature	25 ^o c

The characteristics of this module are shown in figure 3 and 4. Figure 3 shows the current vs. voltage curve for a PV module at different irradiance. Figure 4 shows the power vs. voltage curve for a PV module at different irradiance.

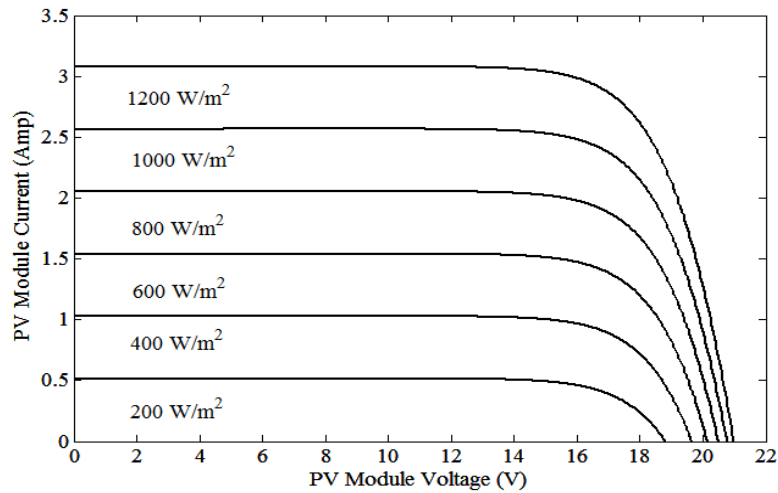


Figure 3. I-V Characteristic at different irradiance

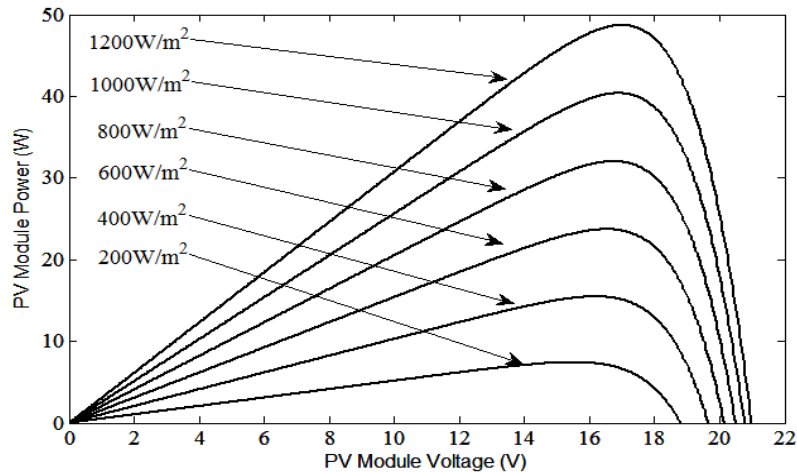


Figure 4. P-V curve at different irradiance

3. MAXIMUM POWER POINT TRACKING

There are many algorithms for maximum power point tracking. Among them P & O is most widely used algorithm. It is a kind of “hill-climbing” method. In figure 4 P-V curve is shown. In this curve, on the right side of MPP the change in power with respect to voltage $dP/dV < 0$ and on the left $dP/dV > 0$ [9].

If the operating voltage is perturbed in certain direction, if $dP/dV > 0$ the panels operating point is moved closer to MPP. If $dP/dV < 0$ the operating point of the panel moves away from the MPP. Then P & O algorithm reverses the direction of perturbation [10]. The P & O method is easy to implement and it needs lesser calculation. However, it has some disadvantages such as slow response, wrong tracking under rapid changing atmospheric condition and oscillation around MPP [10]-[12]. The flow chart of the implemented P & O algorithm is illustrated in Figure (5)

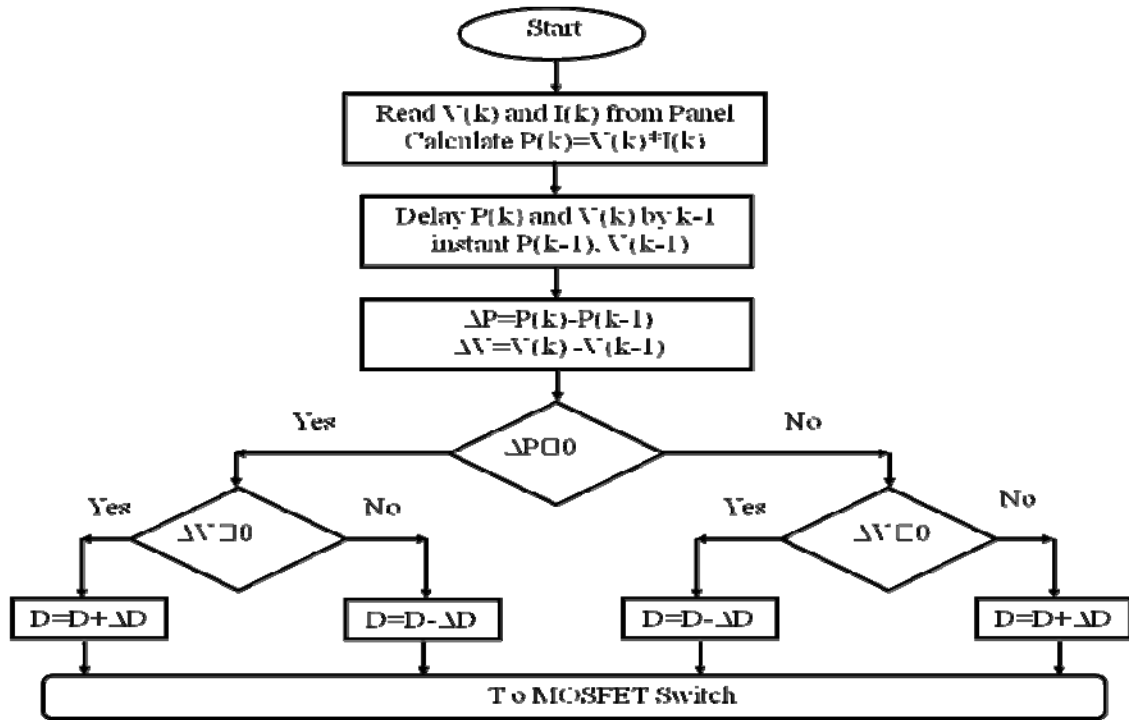


Figure 5. Flowchart of implemented P & O algorithm

The algorithm works in this way. Present power $P(k)$ is calculated using present voltage $V(k)$ and current $I(k)$. Then it is compared with the previous power $P(k-1)$. If the power increases, the voltage is changed in the same direction. Otherwise the voltage direction is changed.

4. NON-INVERTING BUCK-BOOST CONVERTER:

A non-inverting buck-boost converter is essentially a cascaded combination of a buck converter followed by a boost converter, where a single inductor-capacitor is used for both [13]. As the name implies, this converter does not invert the polarities of the output voltage in relation to the polarities of the input. This converter requires the use of two active switches and is designed by combining a buck converter and boost converter design in the same topology. Due to this design this converter can work as Buck-only, Boost-only or Buck-Boost converter. The input voltage source is connected in parallel with diode $D1$, MOSFET S_{boost} , load capacitor, C as indicated in Figure 6. MOSFET S_{buck} is connected between the input voltage source and diode $D1$. The inductor is connected between $D1$ and S_{boost} , while $D2$ is connected between S_{boost} and the output or load capacitor.

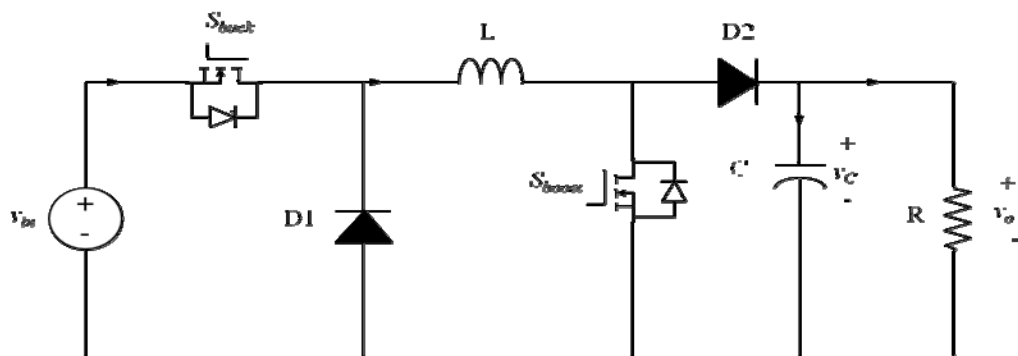


Figure 6. Two switch non-inverting buck-boost converter

4.1. Operation of Non-Inverting Buck-Boost Converter:

In this topology the converter will be operated either in buck mode or boost mode depending upon the load condition. In buck-only mode, S_{buck} is used as a switch, with the diode D1. S_{boost} is turned OFF and diode D2 is always ON. S_{buck} and D1 form the buck switching leg [14]. Figure 7 shows the converter operating at buck mode.

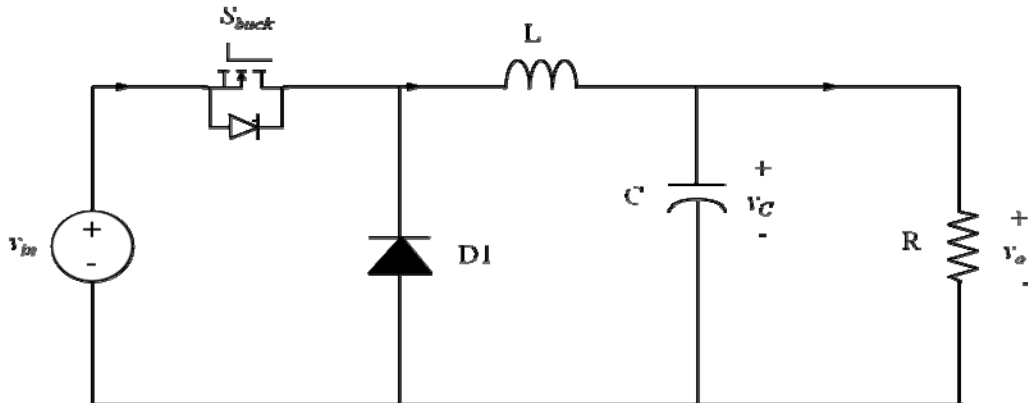


Figure 7. Converter operating at buck mode

When the converter is operated at boost mode then, the switch S_{buck} remains close. In boost-only mode S_{boost} is used as a switch and D2 acts as the diode in the boost regulator. S_{buck} is always ON and D1 is turned OFF. S_{boost} and D2 form the boost switching leg [14]. Figure 8 shows the circuit diagram of the buck boost converter operating at boost mode.

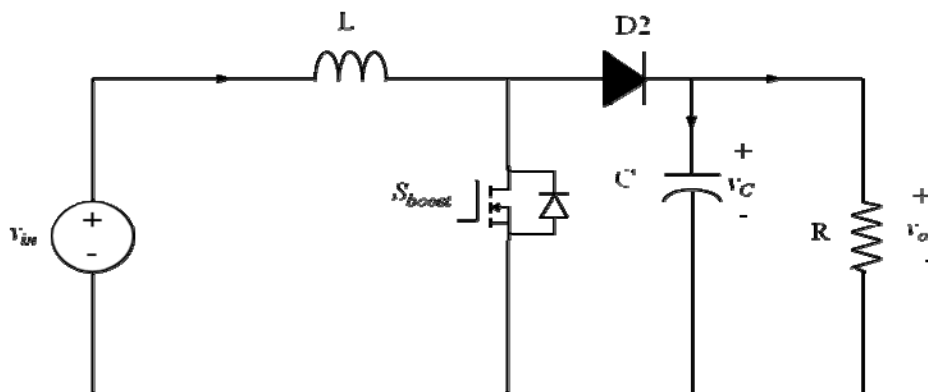


Figure 8. Converter operating at boost mode

In buck-boost mode the S_{buck} and S_{boost} are simultaneously ON during the switching cycle or ON time, while D1 and D2 are simultaneously ON during the opposite switching cycle or OFF time. This means that when S_{buck} and S_{boost} are turned ON, the inductor is getting charged, so D1 and D2 are turned OFF. Vice versa when D1, D2 are ON, the inductor is charging the load capacitor, so S_{buck} and S_{boost} are turned OFF [14].

4.2. Design & Simulation of Non-Inverting Buck-Boost Converter:

The design of non-inverting buck-boost converter is same as the inverting buck-boost converter. The converter is designed considering the data below,

V_{out} = Output voltage = 17.2V

V_D = Diode forward drop = 0.525V

V_{in} = Minimum input voltage = 12V

I_{out} = Average output current = 2.37A

$f =$ switching frequency=20KHz

The calculation starts with the calculation of duty cycle.

The duty cycle can be calculated as:

$$D = \frac{V_{out} + V_D}{V_{out} + V_{in} + V_D}$$

So duty cycle, $D = 0.6$

Ripple Current in the inductor:

$$\Delta I_L = 0.3 \cdot I_L$$

Where, $I_L =$ Average Inductor current $= \frac{I_{out}}{1-D} = 0.4$

$$\Delta I_L = 1.0$$

The inductor of the converter can be found as

$$L = \frac{(V_{in} \cdot D)}{f \cdot \Delta I_L} = \frac{12 \times 0.6}{20 \times 10^3 \times 1.8}$$

So $L = 317 \mu\text{H}$. This is the minimum inductor value for the converter. We choose $600 \mu\text{H}$ as inductance.

The output capacitance can be found from the following equation

$$C_{out} = \frac{I_{out} \cdot D}{(f \cdot \Delta V_{out})} = \frac{2.37 \times 0.6}{20 \times 10^3 \times 0.2}$$

Considering, $\Delta V_{out} =$ Output ripple voltage = 0.2 V , $C_{out} = 355 \mu\text{F}$.

For this experiment we choose $L = 600 \mu\text{H}$ and $C = 470 \mu\text{F}$.

UGP30K and F3205Z are the model number of the diode and MOSFET respectively used in this experiment.

The non-inverting buck-boost converter is simulated using SIMULINK. The values for the components are set as above.

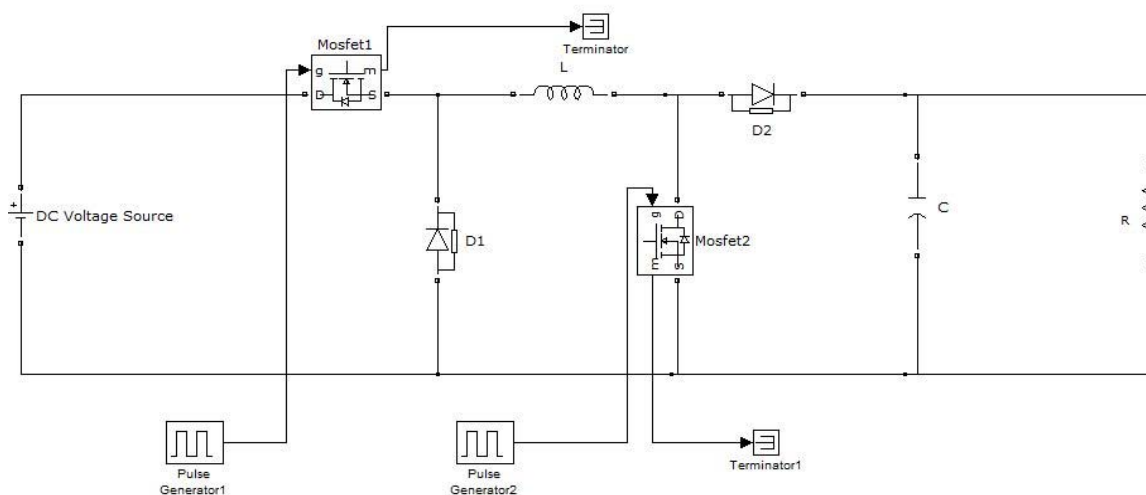


Figure 9. Simulation of non-inverting Buck-boost converter

Figure 9 shows the simulation model of non-inverting buck-boost converter and the output at 60% duty cycle for both buck and boost operation and ripple voltage is shown in figure 10 and 11 respectively. Input voltage was taken as 20V.

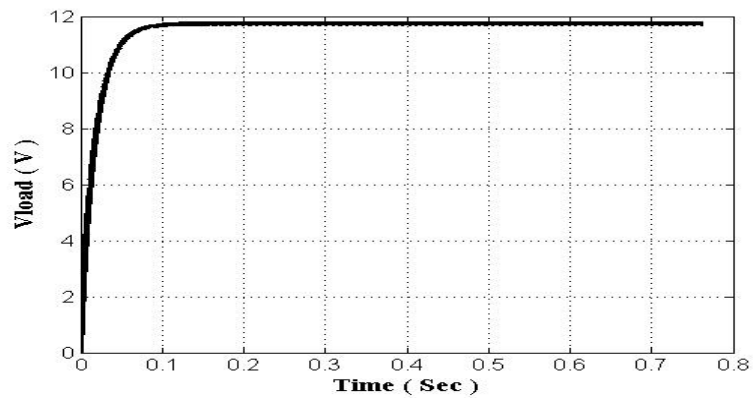


Figure 10. Output voltage of non-inverting buck- boost converter operating at buck mode at 60% duty cycle

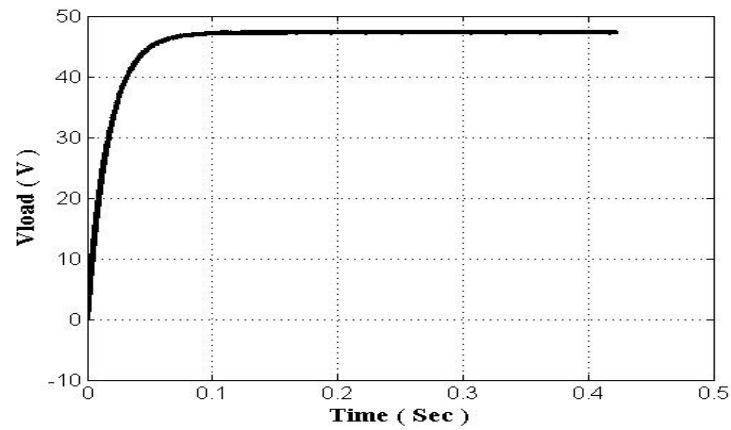


Figure 11. Output voltage of non-inverting buck -boost converter operating at boost mode at 60% duty cycle

Also the ripple voltage is very small about 0.1 V as shown in figure 12.

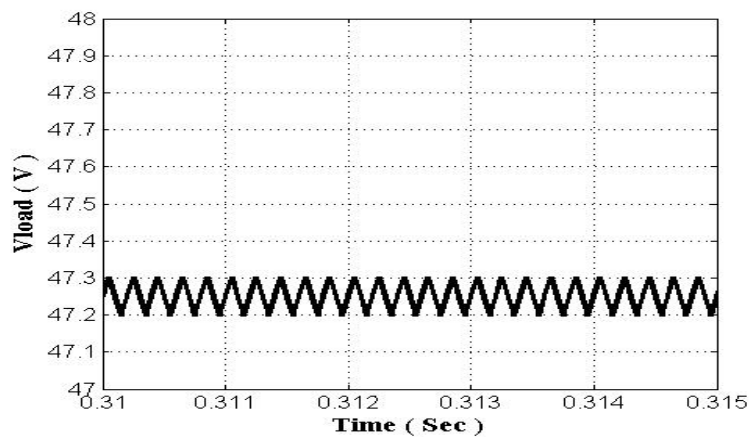


Figure 12. Output ripple voltage of non-inverting buck boost converter

5. PERFORMANCE ANALYSIS

Schematic diagram of the proposed MPPT system is shown in figure 13. Voltage sensor circuit and current sensor circuit are used to sense voltage and current respectively. Outputs of these circuits are sent to microcontroller, which in turn controls the MOSFET according to the algorithm.

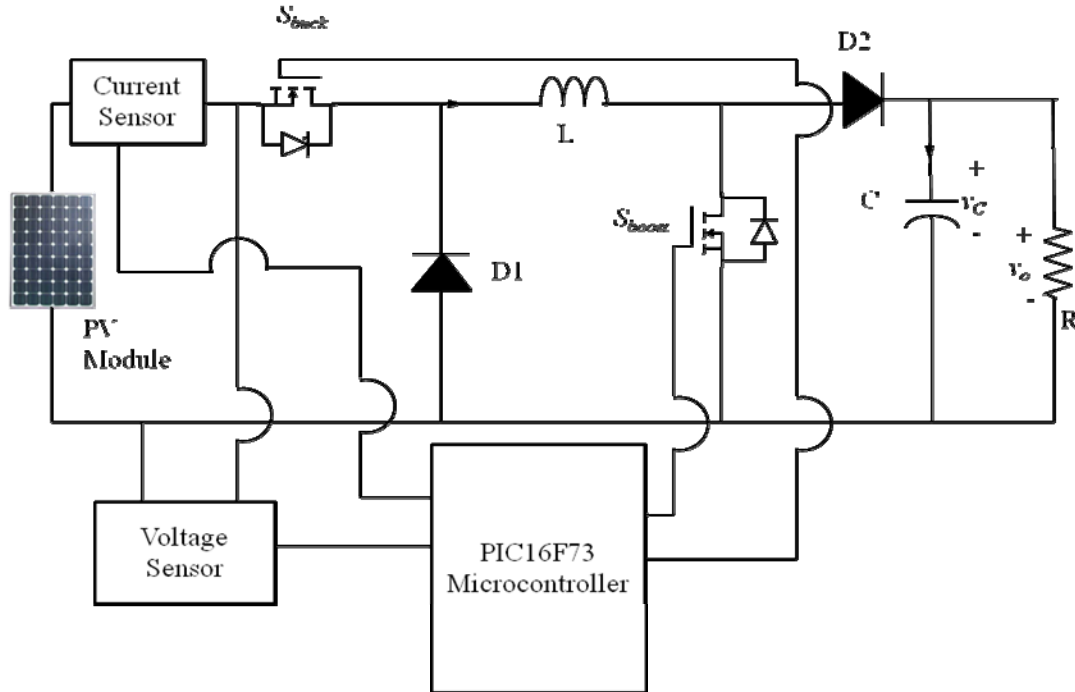


Figure 13. Schematic diagram of the proposed MPPT system

Connecting a load of 4 ohm resistance to the PV module via converter we get

Input Voltage= 12.5 V

Input current=1.25 A

Input power= 12.5*1.25= 15.6W

Output power= 14.8W

So the converter efficiency = $(14.8/15.6)*100$
= 94.88%

So the designed converter is highly efficient.

Output power with and without MPPT is compared to show the difference as shown in table 2. Different power to load is due to different illumination. The output power from the PV module is strongly dependant on irradiation. The implemented circuit diagram of the proposed MPPT system is shown in figure 14.

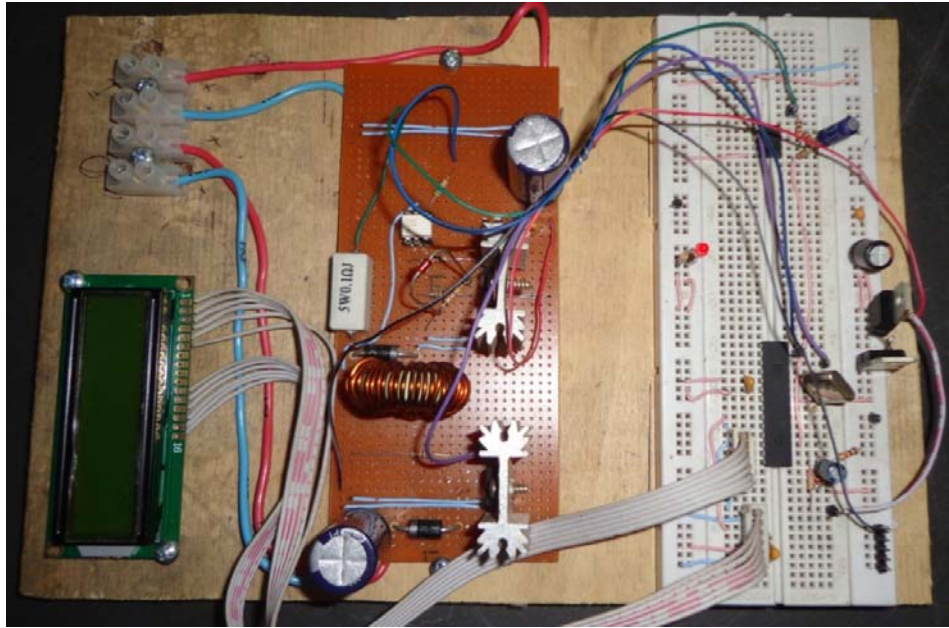


Figure 14. Implemented Circuit diagram of the proposed MPPT system

Table 2. Comparison of output power with and without MPPT

Load(R) Ω	Output Power without MPPT (W)	Output Power with MPPT (W)
4.1	12.4	13.8
6.3	15.18	15.9
7.3	18.2	18.6
11.6	15.41	16.3
17.3	13.125	14.8

The ratio of voltage and current at maximum power point is 7.25 ohm. When load is connected to the PV module for 7.3 ohm and 6.3 ohm, load power is almost same for with MPPT and without MPPT. But when the load is greater or smaller than 7.25 ohm we get greater power with MPPT compared to without MPPT.

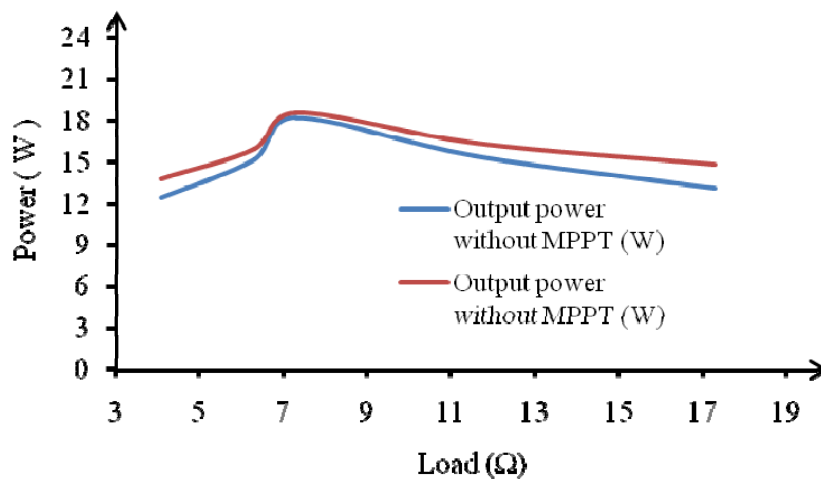


Figure 15. Comparison of power availability

Figure 15 is plotted using the data in table II. It can be seen from the figure that above and below the 7.3 ohm load the output power without MPPT is significantly reduced compared to the output power with MPPT.

6. CONCLUSION

This work proposes a two-switch non-inverting buck-boost converter based Maximum Power Point Tracking System. The proposed converter is about 94% efficient. A greater output power is achieved when MPPT system is connected to the load compared to load without MPPT system. So for higher loads low cost MPPT system could be a better choice to get maximum available power from the solar module.

REFERENCES

- [1] Riza M, Minwon P, Mohammed D, Kenji M, Akira T, Masakazu M (2003). "A maximum power point tracking for photovoltaic-SPE system using a maximum current controller". *Solar Energy Materials and Solar Cells*. 2003; 75: 697-706.
- [2] R Lenk. *Practical Design of Power Supplies*. New York: McGraw-Hill, 1998.
- [3] J Chen, D Maksimovic, R Erickson. "Buck-boost PWM converters having two independently controlled switches". *Power Electronics Specialists Conference, 2001. PESC. 2001*. 2001; 2: 736-741.
- [4] M Veerachary and KS Shinoy. "V2-based power tracking for nonlinear PV sources". *IEE Proceedings-Electric Power Applications*. 2005; 152(5): 1263-1270.
- [5] IS Kim and MJ Youn. "Variable-structure observer for solar array current estimation in a photovoltaic power-generation system". *IEE Proceedings-Electric Power Applications*. 2005; 152(4): 953-959.
- [6] IS Kim, MB Kim, and MJ Youn. "New maximum power point tracker using sliding-mode observer for estimation of solar array current in the grid-connected photovoltaic system". *IEEE Transaction on Industrial Electronics*. 2006; 53(4): 1027-1035.
- [7] KH Hussein, I Muta, T Hoshino, and M Osakada, "Maximum photovoltaic power tracking: an algorithm for rapidly changing atmospheric conditions". *IEE Proceedings of Generation, Transmission and Distribution*. 2005; 142(1): 953-959.
- [8] "MSX-40 Photovoltaic Modules," Solarex, 1997.
- [9] X Weidong, WG Dunford. "A modified adaptive hill climbing MPPT method for photovoltaic power systems". *Power Electronics Specialists Conference PESC 04*. 2004; 3(20-25): 1957-1963.
- [10] DP Hohm, ME Ropp. "Comparative Study of Maximum Power Point Tracking Algorithms Using an Experimental, Programmable, Maximum Power Point Tracking Test Bed". *Photovoltaic Specialists Conference, 2000. Conference Record of the Twenty-Eighth IEEE*. 2000: 1699-1702.
- [11] N Femia, G Petrone, G Spagnuolo and M Vitelli. "Optimizing sampling rate of P&O MPPT technique". *Power Electronics Specialists Conference, PESC04*. 2004; 3: 1945-1949.
- [12] A Brambilla, M Gambarara, A Garutti and F Ronchi: "New approach to photovoltaic arrays maximum power point tracking". *Power Electronics Specialists Conference, PESC 99*. 1999; 2: 632-637.
- [13] RW Erickson. *Fundamentals of Power Electronics*. 1st ed. New York: Chapman and Hall, 1997.
- [14] AN-2124, available at <http://www.national.com/an/AN/AN-2124.pdf> (2 March, 2013)